
Article:
Yang Lim, J., McGregor, J. orcid.org/0000-0001-6813-306X, Sederman, A.J. et al. (1 more author) (2016) The role of the Boudouard and water-gas shift reactions in the methanation of CO or CO2 over Ni/γ-Al2O3 catalyst. Chemical Engineering Science, 152. pp. 754-766. ISSN 1873-4405

https://doi.org/10.1016/j.ces.2016.06.042

The role of the Boudouard and water-gas shift reactions in the methanation of CO or CO_2 over ni/γ-Al_2O_3 catalyst

Jin Yang Lim, J. McGregor, A.J. Sederman, J.S. Dennis

Chemical Engineering Science

www.elsevier.com/locate/ces

PII: S0009-2509(16)30338-4
DOI: http://dx.doi.org/10.1016/j.ces.2016.06.042
Reference: CES13022

To appear in: *Chemical Engineering Science*

Received date: 7 April 2016
Revised date: 14 June 2016
Accepted date: 18 June 2016

Cite this article as: Jin Yang Lim, J. McGregor, A.J. Sederman and J.S. Dennis The role of the Boudouard and water-gas shift reactions in the methanation of CO or CO_2 over ni/γ-Al_2O_3 catalyst, *Chemical Engineering Science* http://dx.doi.org/10.1016/j.ces.2016.06.042

The Role of the Boudouard and Water-gas Shift Reactions in the Methanation of CO or CO_2 over Ni/γ-Al_2O_3 Catalyst

Jin Yang Lim[1], J. McGregor[2], A. J. Sederman[1], J. S. Dennis[1]

[1] Department of Chemical Engineering and Biotechnology, University of Cambridge, Cambridge CB2 3RA, United Kingdom.

[2] Department of Chemical and Biological Engineering, University of Sheffield, Mappin Street, Sheffield S1 3JD, United Kingdom.

Abstract

The Boudouard and the water-gas shift reactions were studied at different temperatures between 453 and 490 K over a Ni/γ-Al_2O_3 catalyst in a Carberry batch reactor using various mixtures of CO, H_2 and CO_2. The activity of the Boudouard reaction was found to be low, compared to the water-gas shift reaction, and diminished over time, suggesting that the temperature was too low for significant activity after an initiation period of CO adsorption. Furthermore, the rate of the Boudouard reaction has been reported to decrease in the presence of H_2O and H_2. The water-gas shift reaction was found to be the main reaction responsible for the production of CO_2 in a mixture of CO, H_2 and H_2O in the batch reactor. The ratio of the total amount of CO consumed to the total amount of CO_2 produced showed that the catalyst was also active towards hydrogenation, where the rate of the hydrogenation reaction was very much faster than the water-gas shift reaction. The resulting ratio of p_{H_2} to p_{CO} was found to be extremely low, probably leading to the production of long-chain hydrocarbons. The stoichiometry of the overall reaction was such that for every mole of mole of CO_2 produced, 1.5 mole of CO was consumed in the batch reactor. Kinetic studies were performed in the batch reactor. An Eley-Rideal mechanism was found to provide a good agreement with the experimental results over a wide range of partial pressures of steam and CO.

1. Introduction

The purpose of the research described in this paper was to ascertain the role of the water-gas shift and Boudouard reactions in consuming CO, in situations where the primary focus was on methanating either CO or CO_2 over Ni/Al_2O_3 catalyst at temperatures below ~490 K. Our previous work (Lim et al. 2016a) has shown that the methanation of CO_2 over a reduced 12 wt% Ni/Al_2O_3 catalyst is extremely selective towards the production of CH_4. Using the same catalyst, the methanation of CO in batch, compared with the methanation of CO_2, is less selective towards CH_4 with some CO_2 being produced (Lim et al. 2012b). The objective of the present paper is to determine the origin of the production of the CO_2. That aside, the water-gas shift and Boudouard reactions are important side reactions in many catalytic processes and therefore understanding them is of some importance.

The two most likely reactions for the production of CO_2, in the presence of CO, are

$$CO_{(g)} + H_2O_{(g)} \rightleftharpoons CO_{2(g)} + H_{2(g)} \quad (1)$$

$$2CO_{(g)} \rightleftharpoons C_{(s)} + CO_{2(g)} \quad (2)$$

Reactions (1) and (2) are, respectively, the water-gas shift and Boudouard reactions, with $K_{P,WGS}$ and $K_{P,BD}$ being the respective equilibrium constants. A number of researchers have examined these reactions. For example, Xu and Froment (1989) observed that the reverse water-gas shift reaction was active at temperatures of 573 – 673 K over a $Ni/MgAl_2O_4$ catalyst. Li et al. (2000) studied the reaction of CO and H_2O over the range 448 – 573 K at atmospheric pressure. They also found the forward water-gas shift reaction to be significant when the catalyst was nickel supported on cerium oxide.

However, several investigations (Tøttrup, 1976; Rostrup-Nielsen and Trimm, 1977; Gardner and Bartholomew, 1981) have found nickel-based catalysts also to be active in the Boudouard reaction, especially in the absence of H_2O. Tøttrup (1976) studied Reaction (2) over reduced 9.9 wt% Ni/Al_2O_3 using a thermogravimetric analyser (TGA). Experiments were performed at temperatures 553 – 633 K at atmospheric pressure. The rate of reaction was determined from the change in mass of the nickel catalyst, as a result of the accumulation of carbon on its surface. Tottrup (1976) noticed an induction period, during which there was a slow initial increase in the mass of the sample, followed by a more rapid, constant increase. This was also observed by Gardner and Bartholomew (1981) who also studied the Boudouard reaction using a TGA at temperatures of 573 – 748 K at atmospheric pressure. Gardner and

Bartholomew (1981) found no increase in the mass of the sample for the first 2 hours, followed by an increase in the rate of deposition of carbon until a constant rate was observed. The induction period was attributed to the dissociative adsorption of CO and the formation of the first 2-3 monolayers of carbon. It was proposed that the formation of the first few layers formed additional surface area on which more carbon could form. This was supported by Rostrup-Nielsen (1972), who observed, using an electron microscope, carbon whiskers on nickel catalyst which had been exposed to CO at 773 K. The rate of accumulation of carbon on the surface of nickel catalysts was found by Gardner and Bartholomew (1981) and Tøttrup (1976) to be a function of the partial pressure of CO, H_2 and H_2O. Both investigations discovered that the rate of accumulation of carbon increased with the partial pressure of CO and decreased in the presence of H_2 and H_2O.

Although the foregoing is primarily concerned with kinetics, it is worth examining Reactions (1) and (2) from a thermodynamic standpoint. Here, a closed vessel containing initial mole fractions of CO and H_2O, $x_{CO,0} = 0.5$ and $x_{H_2O,0} = 0.5$ was considered and the overall thermodynamics explored by evaluating the equilibrium composition at which the Gibb's free energy of the system was at its minimum. Figure 1 illustrates the equilibrium composition of CO, CO_2, H_2O, H_2 and CH_4 for different temperatures at 1 bar based on the thermodynamic properties of the gases (Lemmon et al., 2014). The composition of carbon is expressed as an equivalent gas-phase composition. It is clear that at temperatures below 600 K, the formation of carbon is thermodynamically favourable, even in the presence of H_2O as a result of the Boudouard reaction. However, at 600 – 800 K, the water-gas shift appears to be more dominant, evident from the increase in H_2 and decrease of C. In the present paper, all experiments were performed at temperatures below 500 K, so that the sum of $x_{C,eq}$ and $x_{CO_2,eq}$ was essentially the maximum value allowed by the stoichiometry of the active reactions. In general, Figure 1 suggests that the formation of CO_2 is favourable at the temperatures considered. Therefore, it is impossible to determine the significance of these reactions under CO methanation conditions based on thermodynamic arguments alone.

Furthermore, most of the previous investigations of the Boudouard reaction available in the literature have been performed at temperatures above 550 K; significantly higher than the temperatures of interest in the present work. The investigations by Li et al. (2000) suggested that the water-gas shift reaction was active at temperatures as low as 448 K over a nickel catalyst supported on cerium oxide. However, they did not explore the kinetics of the reaction above atmospheric pressure. The objectives of the research described in this paper were

therefore (i) to determine whether the Ni/Al_2O_3 catalyst is active in either Reactions (1) or (2), or both, and (ii) to study the kinetics of the reactions of interest as a function of different partial pressures of products and reactants, to arrive at a representative rate expression.

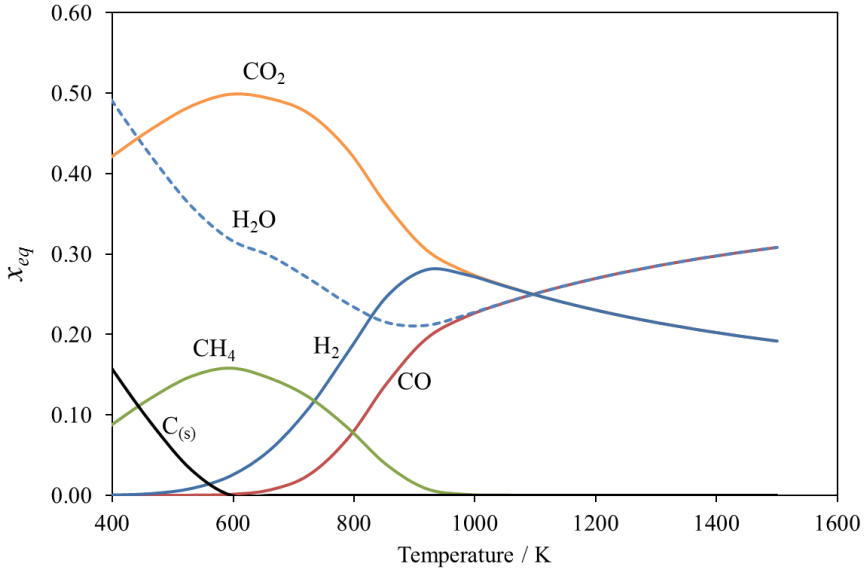

Figure 1. The equilibrium composition of CO, CO_2, H_2, CH_4, H_2O and surface carbon, with an initial composition of $x_{CO,0} = 0.5$ and $x_{H_2O,0} = 0.5$, at different temperatures. The total pressure was 1 bar.

2. Experimental

A reduced 12 wt% Ni catalyst was prepared by the incipient wetness impregnation of pellets of γ-alumina (Saint Gobain – SA 62125, 3 mm dia. spheres) using $Ni(NO_3)_2.6H_2O$ as the precursor salt (Sigma-Aldrich). Details of the synthesis and characterisation have been described in detail by Lim et al. (2016a,b). Information on the surface area and pore size distribution of the catalysts is given in section 1 of the Supplementary Information. A Carberry, spinning basket reactor was used to study the behaviour of the catalyst in the presence of CO, H_2O or both. Gas cylinders of (i) 25 vol% CO_2, 4 vol% Ar, H_2 balance (±1% precision, BOC), (ii) CO (99.5%, BOC), (iii) pure H_2 (99.99%, Air Liquide) and (iv) N_2 (99.998%, Air Liquide) were connected to the reactor. For a typical experiment, 5.0 g of fresh 12wt% Ni/γ-Al_2O_3 was loaded into the basket of the reactor and the catalyst reduced at 523 K in a flow of 100 ml/min H_2 (at room temperature and pressure) for 12 hours (Lim et al. 2016a) before the catalyst was exposed to the other reactive gases, such as CO, H_2 and CO_2. . Full details of the apparatus and method are given in section 2 of the Supplementary Information. The long reduction period was because the maximum operating temperature of the Carberry

reactor was limited to 523 K, thus trading off temperature for time. Full details of the impact of this period of reduction on the structure and properties of the catalyst are given by Lim et al. (2016b).

2.1 Catalyst deactivation

As noted by Lim et al. (2016a,b), no significant deactivation occurred after repeated runs of CO_2 methanation on the same batch of catalyst. Similarly, after its exposure to a mixture of CO, H_2O, CH_4 and H_2, the catalyst did not undergo significant deactivation. Since the present work investigates the water-gas shift and Boudouard reactions, the gases involved in these reactions are similar to those explored in the replicate experiments described in Lim et al. (2016a,b). Therefore, it was inferred that no significant deactivation should occur in the reactions performed in the present work. As a precaution, the same batch of catalyst was used for no more than 10 experiments before being replaced by a fresh batch. CO_2 methanation, performed at the reference condition of $p_{CO_2,0} = 2.4$ bar, $p_{H_2,0} = 2.4$ bar, T = 463 K, was carried out as the final experiment on a batch of catalyst. The results of this final experiment were compared with those presented by Lim et al. (2016a) to verify that no deactivation had occurred over the duration of the previous experiments.

2.2 Heat and mass transfer

The enthalpy of the Boudouard reaction at 298 K is $\Delta H_{298\,K} = -172$ kJ/mol whereas the water-gas shift reaction is only mildly exothermic, with $\Delta H_{298\,K} = -41$ kJ/mol. Whilst the enthalpy of the Boudouard reaction is similar to that of CO_2 methanation, the rates of reactions observed in the experiments described in the present paper were significantly lower than those observed with the methanation of CO_2 (Lim et al. 2016a). Thus, the rate of production of CO_2 in the Carberry reactor with an initial condition of $p_{CO,0} = 2$ bar and $p_{H_2O,0} = 1.8$ bar at 463 K was 8×10^{-5} mol s^{-1} kg^{-1}, less than a tenth of the rate of the production of CH_4 used in the analysis for heat and mass transfer by Lim et al. (2016a), who showed that for the methanation of CO_2 both heat and mass transfer effects both within, and external to, the particle were very small. Therefore, the effects of heat and mass transfer, from the bulk phase of the reactor volume to the surface of the catalyst and within the pores of the catalyst pellet, can be assumed to be negligible in the measurements of the rate of reaction presented in this work.

Since the water-gas shift reaction has an enthalpy of reaction significantly smaller than that of CO_2 methanation, there should be no influence of temperature gradients in kinetic measurements of the water-gas shift reaction.

3. Results

3.1 Behaviour of the reactions in a batch reactor

In order to study the Boudouard reaction, a mixture of 1.5 bar of Ar and 4 bar of CO was introduced into the evacuated Carberry reactor at 463 K. Small samples of gas were removed from the reactor volume for analysis by GC, as described by Lim et al. (2016a). The production of CO_2 could only originate from the reaction of CO with the nickel to form surface carbon and gaseous CO_2, i.e. the Boudouard reaction. Figure 2 illustrates the production of CO_2 over time.

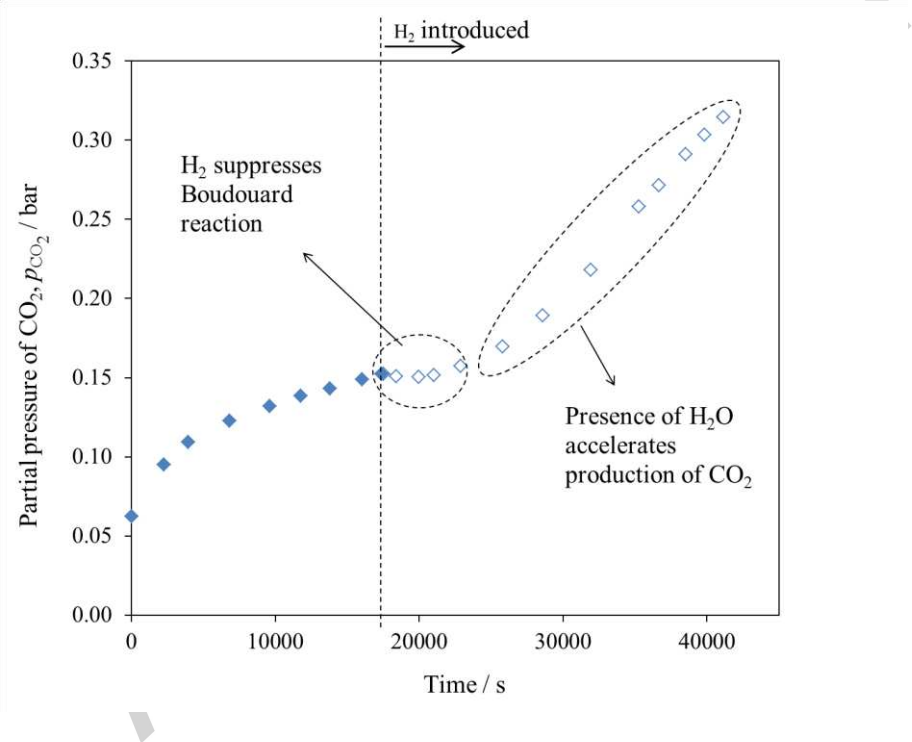

Figure 2. The partial pressure of CO_2 versus time for an initial condition of $p_{CO,0} = 4$ bar and $p_{Ar,0} = 1.5$ bar. At t = 17520 s, 1.0 bar of H_2 was introduced into the reactor. T = 463 K and m_{cat} = 5.0 g. The solid and open symbols represent p_{CO_2} before and after, respectively, the introduction of H_2.

At t = 20 s, about 0.06 bar of CO_2 was detected, followed by a gradual increase of p_{CO_2} over time. The rate of change of p_{CO_2} with time decreased as the reaction proceeded, indicating that the rate of the Boudouard reaction was decreasing. Figure 3 shows that CO

was consumed during this period, at a decreasing rate, suggesting that the Boudouard reaction was active in the presence of CO. It should be noted that a small amount of CH_4, ~ 0.08 bar, was detected just after the introduction of CO into the evacuated reactor. The small decrease in p_{CH_4} can be attributed to the removal of contents from the reactor volume for sampling; accordingly, p_{CH_4} should be treated as a constant for t < 17520 s. This small amount of CH_4 is likely to have been produced from the reaction of CO with residual H_2 on the surface of the catalyst present as a result of the reduction procedure, where the catalyst was reduced in a stream of H_2. After approximately t = 10 000 s, there was negligible decrease in p_{CO} with time, in line with the small increase in p_{CO_2} with time. At 17 520s, p_{CO_2} was approximately 0.15 bar and the total loss of p_{CO} was about 0.5 bar. According to the stoichiometry of Reaction (2), one mole of CO_2 is produced for every two moles of CO consumed in the reaction. The additional loss of about 0.2 bar of CO is attributable to the irreversible adsorption of CO on the surface of the catalyst during the initial exposure to CO.

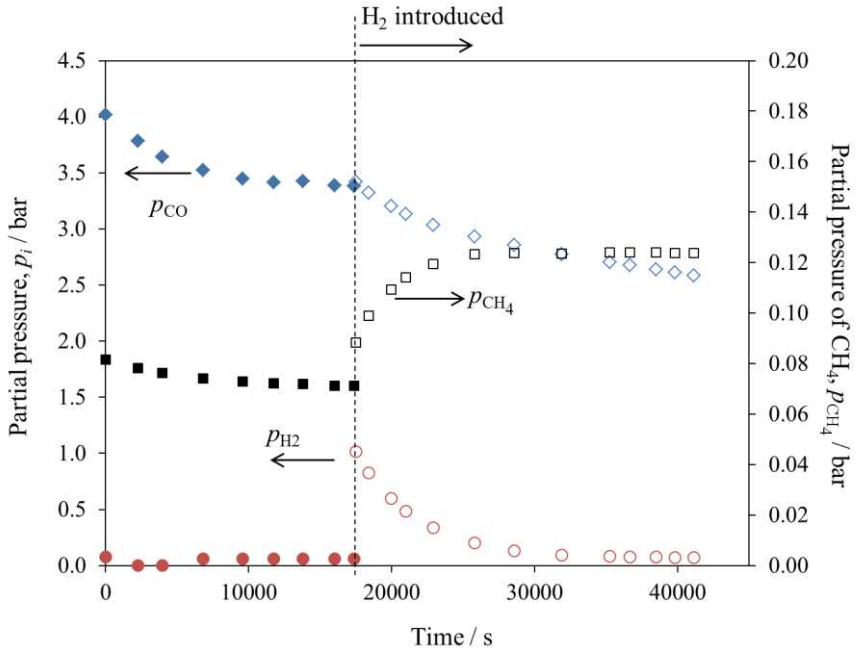

Figure 3. The partial pressure of CO, H_2 and CH_4 versus time for an initial condition of $p_{CO,0} = 4$ bar and $p_{Ar,0} = 1.5$ bar. At t = 17520 s, 1.0 bar of H_2 was introduced into the reactor. T = 463 K and m_{cat} = 5.0 g. The solid and open symbols represent the partial pressures of each species before and after, respectively, the introduction of H_2.

At t = 17520 s, marked by the vertical dotted line in Figures 2 and 3, 1 bar of H_2 was introduced into the reactor. The subsequent variations of the partial pressures of CO_2, CO, H_2

and CH_4 are illustrated by the open symbols in Figures 2 and 3. The rate of production of CO_2 was approximately zero immediately after the introduction of the H_2. However, after a further 8000 s, more CO_2 was produced until a steady rate of production of CO_2 was achieved. Figure 3 shows that both CO and H_2 were consumed in a monotonic manner, indicating that some reactions between CO and H_2, e.g.

$$CO + 3H_2 \longrightarrow CH_4 + H_2O \quad (3)$$

and

$$CO + 2H_2 \longrightarrow -(-CH_2-)-+H_2O, \quad (4)$$

had occurred. Reaction (3) is CO methanation and (4) represents the production of paraffins heavier than methane. This was evident from the marked increase in p_{CH_4} immediately after the introduction of the H_2. It should be noted that after the p_{H_2} had fallen to zero, p_{CO} continued to decrease and p_{CO_2} continued to increase.

The production of CO_2 after the introduction of H_2 was attributed to the water-gas shift Reaction (1), for the following reasons. It has been established, by other researchers (Tøttrup, 1976; Gardner and Bartholomew, 1981), that the presence of H_2 depresses the rate of the Boudouard reaction. This is in agreement with the lack of production of CO_2, in Figure 2, immediately after H_2 was introduced at t = 17520 s. The initiation of Reactions (3) and (4) led to the production of H_2O which reacted with CO to form CO_2. The increasing rate of production of CO_2 after the introduction of H_2 suggests that p_{H_2O} has a positive order in the rate expression for the water-gas shift reaction. This is confirmed, below, where the rate of the water-gas shift reaction was measured for different p_{H_2O} and p_{CO}. It is interesting to note that while ~ 1 bar of H_2 was consumed in Figure 3, only 0.04 bar of CH_4 was produced, far less than expected if CO and H_2 were consumed via reaction (3) only. The extremely low ratio of H_2 to CO probably favoured the production of heavy paraffins, which condensed and therefore could not be detected in the gas samples. This was found to be consistent with the observations of Lim et al. (2016b), where it was found in the methanation of CO that a low ratio of the partial pressure of H_2 to CO favours the production of heavier hydrocarbons.

Further evidence that the reduced 12 wt% Ni/γ-Al_2O_3 was active in the water-gas shift reaction is shown in Figures 4 and 5. In the experiment shown, using the method described in Lim et al. (2016a), CO_2 methanation was performed to completion in the Carberry reactor in batch at 483 K to form approximately 0.6 bar of H_2O and 0.3 bar of CH_4. The reaction was deemed complete when no further decrease in the total pressure of the batch reactor,

measured by two pressure gauges, was detected for 1800 s. At this point, 4 bar of CO was introduced into the reactor and the gaseous composition of the contents of the reactor was analysed periodically. The instant at which CO was introduced into the reactor was taken as t = 0 s in Figures 4 and 5. In this way, the reaction between H_2O and CO was studied. Figure 4 shows that p_{CO_2} increased immediately after the introduction of CO. This is in contrast to the behaviour of p_{CO_2} in Figure 2, where a delay was observed after the introduction of H_2. For the experiment illustrated in Figure 4, very little H_2 was present at t = 0s. Hence, the decrease in p_{CO} with time was postulated to be the result of CO reacting via the water-gas shift reaction to form CO_2. The rate of reaction, deduced from the rate of change of p_{CO_2} and p_{CO} with time, decreased as the reaction proceeded. As mentioned previously, this suggests that the rate of the water-gas shift reaction is positively influenced by p_{H_2O}. After 1×10^5 s, the rate of reaction appeared to have dropped to approximately zero, suggesting that p_{H_2O} was depleted and confirming that the presence of H_2O is necessary for the production of CO_2. The production of CO_2 after 1×10^5 s at a low rate can probably be attributed to the Boudouard reaction, which appeared to be significantly slower than the water-gas shift at these conditions.

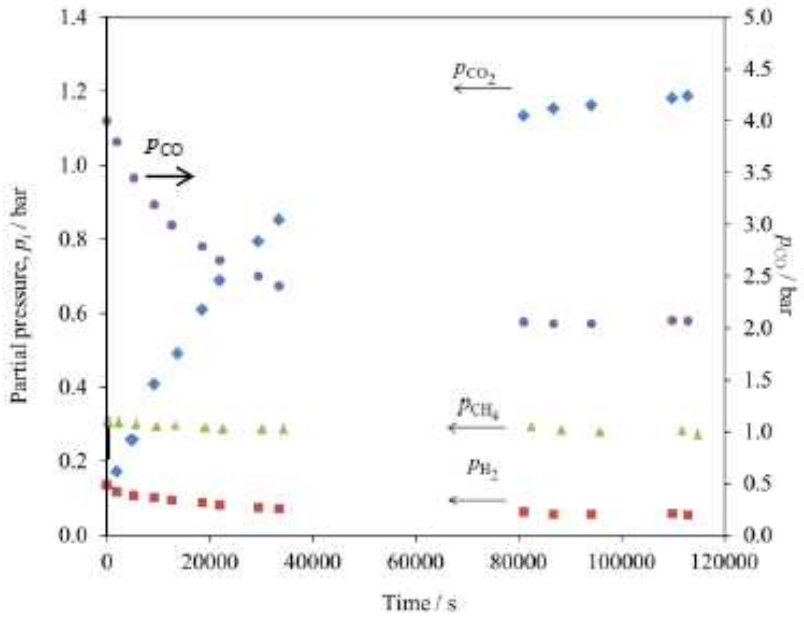

Figure 4. The partial pressure of CO, CO_2, CH_4 and H_2 versus time for an initial condition of $p_{CO,0} = 4$ bar and $p_{H_2O,0} = 0.6$ bar. T = 483 K and m_{cat} = 5.0 g.

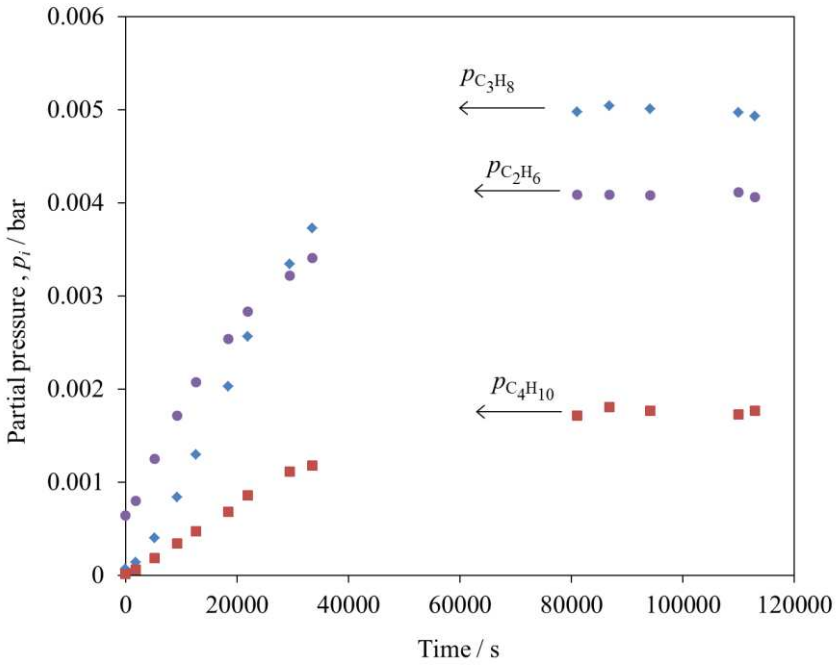

Figure 5. The variation of the partial pressures of C_2H_6, C_3H_8 and C_4H_{10} as a function of the time an initial condition of $p_{CO,0} = 4$ bar and $p_{H_2O,0} = 0.6$ bar . T = 483 K and m_{cat} = 5.0 g.

Is it interesting to note that, in Figure 4, the total amount of CO consumed, as measured by change in p_{CO}, exceeded the total amount of CO_2 produced, as measured by change in p_{CO_2}, thus giving an apparent discrepancy in the carbon balance. Over the duration of the reaction, approximately 1.9 bar of CO was consumed and only about 1.2 bar of CO_2 was produced. Furthermore, if the water-gas shift reaction were the only reaction, p_{H_2} should have increased since H_2 is a product of the reaction. However, Figure 4 clearly shows little variation in p_{H_2} over time. It is known that nickel catalysts are active in hydrogenation and methanation reactions with CO, therefore it is postulated here that the H_2 produced from the water-gas shift reaction was immediately consumed in either reaction (3) or (4). This would be true if the rate of these hydrogenation reactions were much faster than that of the water-gas shift reaction, which is, in fact, the case, as confirmed by Lim et al. (2016a,b). Figure 4 also shows that no increase of p_{CH_4} was found over the duration of the experiment. This was probably the result of the extremely low ratio of partial pressures of H_2 to CO, which shifted the selectivity of the reaction towards the production of heavier hydrocarbons, i.e. via reaction (4). Some evidence for the production of higher alkanes is illustrated in Figure 5, where the partial pressures of C_2H_6, C_3H_8 and C_4H_{10} were found to increase in a similar trend

to that of p_{CO_2}; there was also no further increase in the partial pressures of these species after $t = 8 \times 10^4$ s when p_{H_2O} was depleted. It can be seen that the partial pressures of the gaseous hydrocarbons are extremely small and cannot fully account for the discrepancy in the carbon balance. The bulk of the product is expected to be longer-chained hydrocarbons, which were not detected in the analysis of the gas phase.

To sum up, it is postulated that the reactions in Figures 4 and 5 occurred in the following order. The introduction of CO into the batch reactor initiated the water-gas shift reaction to produce CO_2 and H_2. The rate of the Boudouard reaction was much lower than that of the water-gas shift reaction, especially in the presence of H_2O. Since the rate of the water-gas shift reaction was lower than that of reaction (4), any available hydrogen produced by the water-gas shift reaction was consumed by reaction (4). Hence, only very small amounts of H_2 were present in the bulk phase of the reactor and the ratio of H_2 to CO remained very small. The low ratio of H_2 to CO led to the low selectivity towards CH_4. Furthermore, for every 2 moles of H_2 produced by the water-gas shift reaction, one additional mole of CO was taken up by reaction (4). Assuming that reaction (4) is the dominant hydrogenation reaction, the overall reaction can be expressed as

$$3CO + H_2O \longrightarrow 2CO_2 + -(-CH_2-) - . \quad (5)$$

This explains why more CO was consumed compared to the amount of CO_2 produced, as noted earlier. Furthermore, the total amount of p_{H_2O} consumed at the end of the reaction, illustrated in Figure 4 and 5, was 0.6 bar, a value consistent with the stoichiometry of reaction (5) since about 1.2 bar of CO_2 was produced during the same period. When p_{H_2O} was depleted, both reactions (2) and (4) stopped. The small rate of increase of p_{CO_2} after 8×10^4 s might be the result of the Boudouard reaction, which was expected to resume some activity after the depletion of H_2 and H_2O. Therefore, it seems reasonable to conclude that the water-gas shift reaction is the dominant reaction responsible for the production of CO_2 under typical conditions for CO methanation, where significant p_{H_2} and p_{H_2O} are normally present.

3.2 Reaction kinetics

Since it has been established that the production of CO_2 during CO methanation was the result of the water-gas shift reaction, kinetic measurements of the water-gas shift reaction were undertaken in the Carberry reactor at temperatures between 453 and 498 K. The

following sections describe the effect of p_{H_2O}, p_{CO} and temperature on the rate. It has been established that CO, H_2 and CH_4 participate in both reactions (1) and (4). However, the variation of p_{CO_2} is the result solely of reaction (1), i.e. the water-gas shift reaction. Therefore, the rate of the water-gas shift reaction could be calculated from the rate of change of p_{CO_2} with time.

3.2.1 Effect of p_{H_2O}

As noted earlier, the effect of p_{H_2O} on the water-gas shift reaction was studied in the batch reactor by first performing CO_2 methanation to completion before a known amount of CO was introduced. This amount was measured by the difference in the readings of the pressure gauges before and after the introduction of CO. The composition of the final mixture was also confirmed by gas chromatography. The instant at which CO was introduced into the reactor was taken as t = 0 s.

To study the effects of different p_{H_2O}, various initial partial pressures of CO_2 and H_2 were introduced and the amount of CH_4, H_2O and residual CO_2 remaining in the batch reactor when H_2 had been completely reacted was estimated based on the stoichiometry of CO_2 methanation. For example, with an initial condition of $p_{CO_2,0} = 1.2$ bar and $p_{H_2,0} = 3.6$ bar, the composition of the reactor after CO_2 methanation had proceeded to completion was approximately 0.9 bar of CH_4, 1.8 bar H_2O and 0.3 bar CO_2. Lim et al. (2016a) found that, in the presence of CO, CO_2 is a spectator molecule and does not participate in any reactions because of the strong affinity of CO for the surface of the catalyst.

Figure 6 illustrates the change of p_{CO_2}, p_{CO}, p_{H_2} and p_{CH_4} with time for different initial partial pressures of H_2O. The experiments were performed at 463 K and the initial partial pressure of CO, $p_{CO,0}$, was 2 bar for all experiments. As noted earlier, there was some residual p_{CO_2} at t = 0 s arising from CO_2 methanation. For ease of comparison, Figure 6 (a) plots the net change in p_{CO_2} with time, i.e. $p_{CO_2} - p_{CO_2,0}$ and shows that p_{CO_2} increased at a faster rate for higher $p_{H_2O,0}$: the rate of production of CO_2 increased from $6.1 \times 10^{--5}$ mol s^{-1} kg^{-1} to 1.4×10^{-4} mol s^{-1} kg^{-1} when $p_{H_2O,0}$ was increased from 1.1 bar to 3.6 bar. During the same period, p_{CO} also decreased by ~ 1.5 times the total decrease in p_{CO_2}, illustrated in

Figure 6 (a). This observation is consistent with the stoichiometry of reaction (5) and the observations in Figure 3.

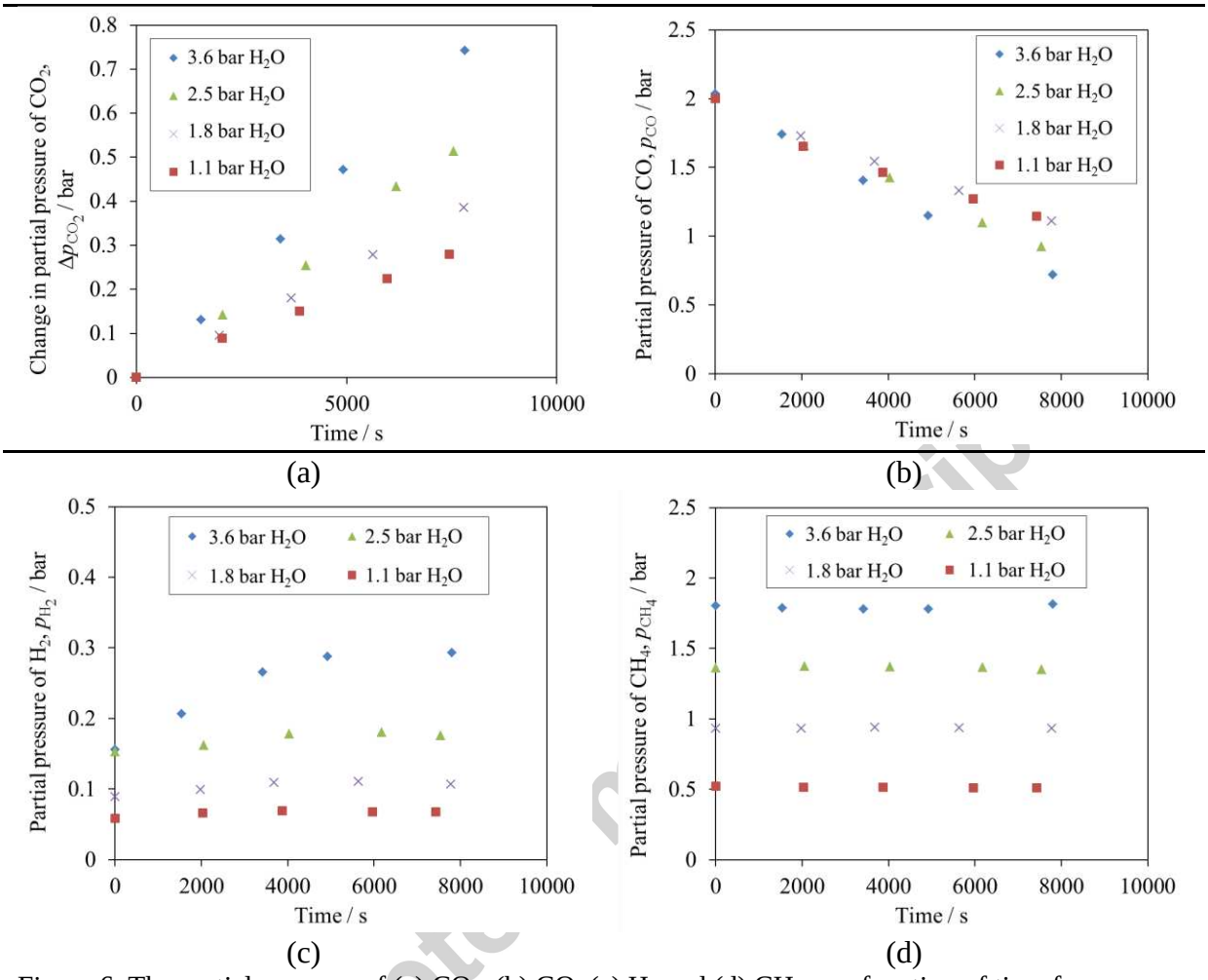

Figure 6. The partial pressure of (a) CO_2, (b) CO, (c) H_2 and (d) CH_4 as a function of time for different initial partial pressure of H_2O, $p_{H_2O,0}$. For all experiments, $p_{CO,0} = 2$ bar, T = 463 K and m_{cat} = 5.0 g.

Figure 6 (c) shows that for $p_{H_2O,0}$ of 1.1 bar and 1.8 bar, there was very little variation in p_{H_2} after the introduction of CO, suggesting that the rate of consumption of H_2 by reaction (4) is approximately equal to the rate of production of H_2 by the water-gas shift reaction. However, at higher $p_{H_2O,0}$ of 2.5 and 3.6 bar, a small increase in p_{H_2} was observed, suggesting that the increased rate of the water gas shift reaction is faster than the consumption of H_2 by reaction (4) under these conditions. At 463 K, no increase in p_{CH_4} with time was observed for all explored $p_{H_2O,0}$, as illustrated in Figure 6 (d). This shows that the selectivity of the catalyst favoured reaction (4) over reaction (3).

The effect of different values of $p_{H_2O,0}$ was explored for temperatures 453, 463 and 488 K. At 453 K, the general trends of p_{CO}, p_{H_2} and p_{CH_4} with time were similar to those observed in Figure 6, viz. p_{H_2O} increases the rate of the water-gas shift reaction and no change in p_{H_2} and p_{CH_4} were observed. However, at the higher temperature of 488 K, some variations were observed in the change of p_{H_2} and p_{CH_4} with time. Figure 7 illustrates the experimental measurements for different $p_{H_2O,0}$ at 488 K. In general, the rate of production of CO_2 and the corresponding consumption of CO was faster for higher $p_{H_2O,0}$, as observed at all other temperatures. However, Figure 7 (d) shows that some CH_4 was being produced by the catalyst over the duration of the experiment. The value of p_{H_2} also appeared to increase slightly during the initial phase of the reaction, i.e. for $t < 2500$ s, before dropping, as shown in Figure 7 (c). This behaviour is especially obvious at high $p_{H_2O,0}$. A higher p_{H_2} was produced probably because of a faster initial rate of the water-gas shift reaction at higher p_{H_2O}. As more H_2 was present in the bulk phase of the reactor, the rate of reactions (3) and (4) increased, explaining the subsequent drop in p_{H_2} after having reached a maximum value. The relationship between the rates of reactions (3) and (4) with p_{H_2} is confirmed by the findings of Lim et al. (2016b), where the rate of CO methanation was found to be a positively correlated with increases in p_{H_2}. The increase in p_{CH_4} seen in Figure 7 (d) at 488 K, but not observed at 463 K, suggests that the catalyst was more selective towards reaction (3) at higher temperatures. Furthermore, since the overall rate of reaction was faster at higher temperatures, p_{CO} also reached a lower level in 8000 s, which is the typical duration of an experiment. Since the variations in p_{H_2} were generally small in absolute partial pressures, lower p_{CO} led to a slightly higher ratio of H_2 to CO, which also favoured the production of CH_4.

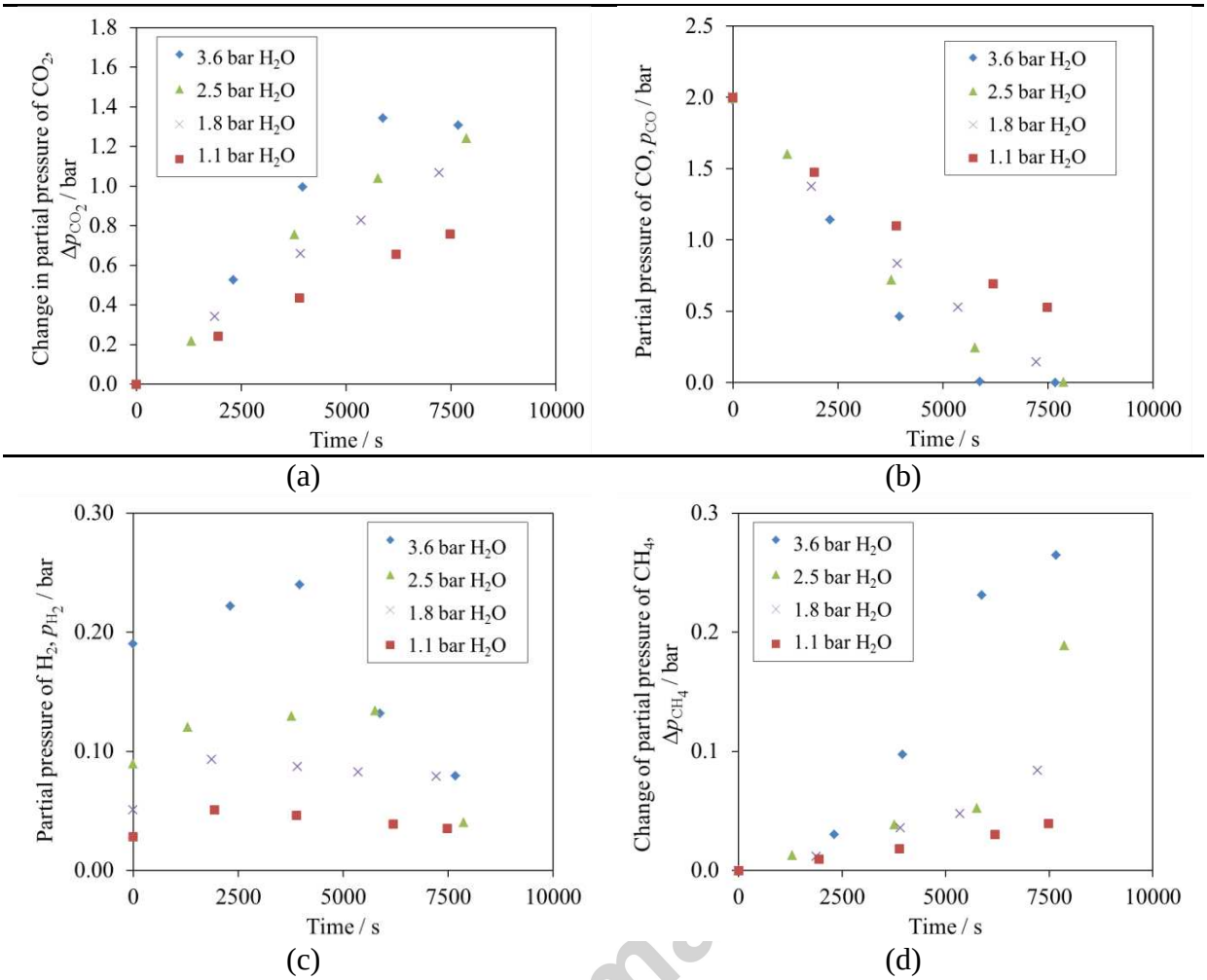

Figure 7. The partial pressure of (a) CO_2, (b) CO, (c) H_2 and (d) CH_4 as a function of time for different initial partial pressure of H_2O, $p_{H_2O,0}$. For all experiments, $p_{CO,0} = 2$ bar, T = 488 K and m_{cat} = 5.0 g.

3.2.2 Effect of p_{CO}

Figure 8 shows the variation of the partial pressures of CO_2, CO, H_2 and CH_4 for different initial partial pressures of CO, $p_{CO,0}$, for a fixed initial partial pressure of H_2O, $p_{H_2O,0}$, at 463 K. Figure 8 (a) shows that the initial rate of production of CO_2 was largely unaffected by variations in $p_{CO,0}$ and was found to be approximately 7.7×10^{-5} mol s^{-1} kg^{-1}. Figure 8 (b) shows the net change of the partial pressure of p_{CO}, i.e. $p_{CO} - p_{CO,0}$, with time. For $p_{CO,0} = 0.25$ bar and $p_{CO,0} = 0.50$ bar, p_{CO} was depleted after approximately 4000 s and 6000 s respectively. Figure 8 (a) shows that, after these times, no further increase in p_{CO_2} was observed. It also shows that the rate of reaction changed very abruptly from a constant

rate, before p_{CO} was depleted, to a rate of zero. The variations of p_{H_2} and p_{CH_4} with time are illustrated in Figures 8 (c) and (d). Only small changes in p_{H_2} were observed before p_{CO} was depleted and slightly more CH_4 was produced for $p_{CO,0} = 0.25$ bar compared to $p_{CO,0} \geq 0.50$ bar. The general behaviour of p_{H_2} and p_{CH_4} were largely consistent with observations discussed in Section 3.2.1.

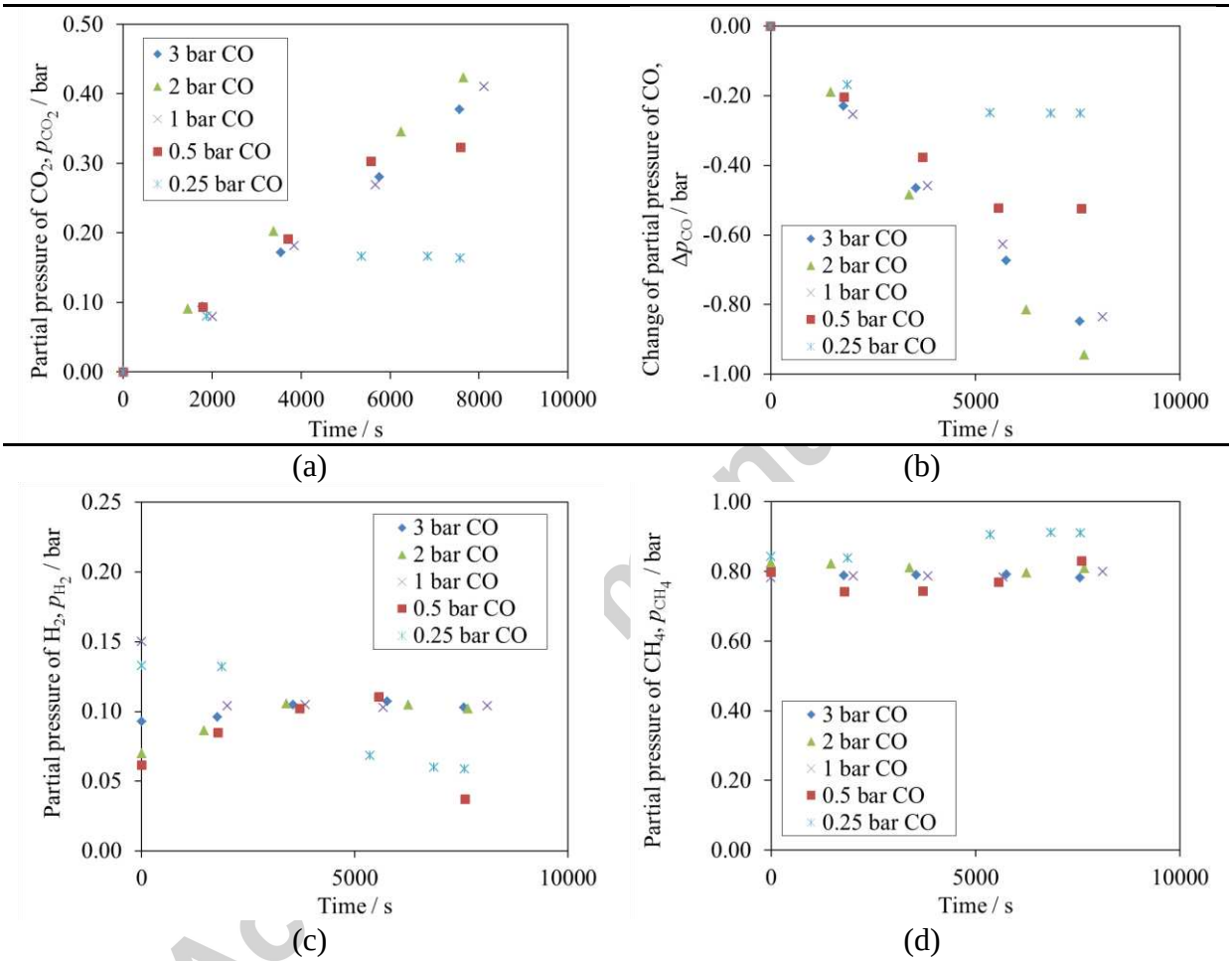

Figure 8. The partial pressure of (a) CO_2, (b) CO, (c) H_2 and (d) CH_4 as a function of time for different initial partial pressure of CO, $p_{CO,0}$. For all experiments, $p_{H_2O,0} = 1.8$ bar, T = 463 K and m_{cat} = 5.0 g.

3.2.3 Effect of temperature

Figure 9 shows the partial pressures of CO_2, CO, H_2, CH_4 and C_2H_6 as a function of time for different reaction temperatures, with initial conditions of $p_{H_2O,0} = 1.8$ bar and $p_{CO,0} = 2$ bar. In general, the rate of production of p_{CO_2} was faster at higher temperatures,

illustrated in Figure 9 (a), viz. the rate of the water-gas shift reaction increased with temperature. The corresponding decrease of p_{CO} for different temperature is also shown in Figure 9 (b). The change in p_{H_2}, shown in Figure 9 (c), shows the interaction between the differences in the rate of the water-gas shift reaction and the hydrogenation reactions, such as reactions (3) and (4). This is evident from the presence of a maximum p_{H_2} for temperatures 463 – 498 K. Figures 9 (d) and (e) show that the rate of production of CH_4 and C_2H_6, as measured by their partial pressures, increased with temperature. This suggests that the catalyst is more selective towards the production of lighter alkanes at higher temperatures. However, at higher temperature, the consumption of CO was also faster leading to a higher ratio of p_{H_2} to p_{CO}, which also favours the production of light hydrocarbons.

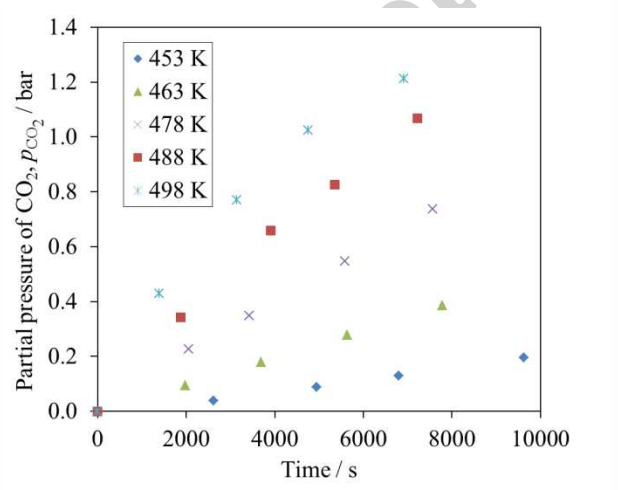

(a)

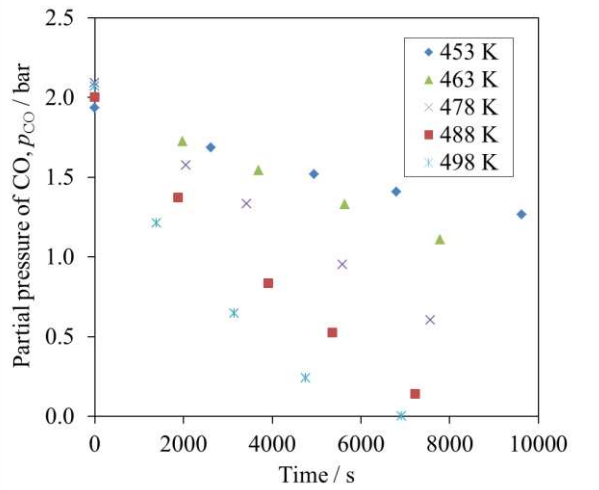

(b)

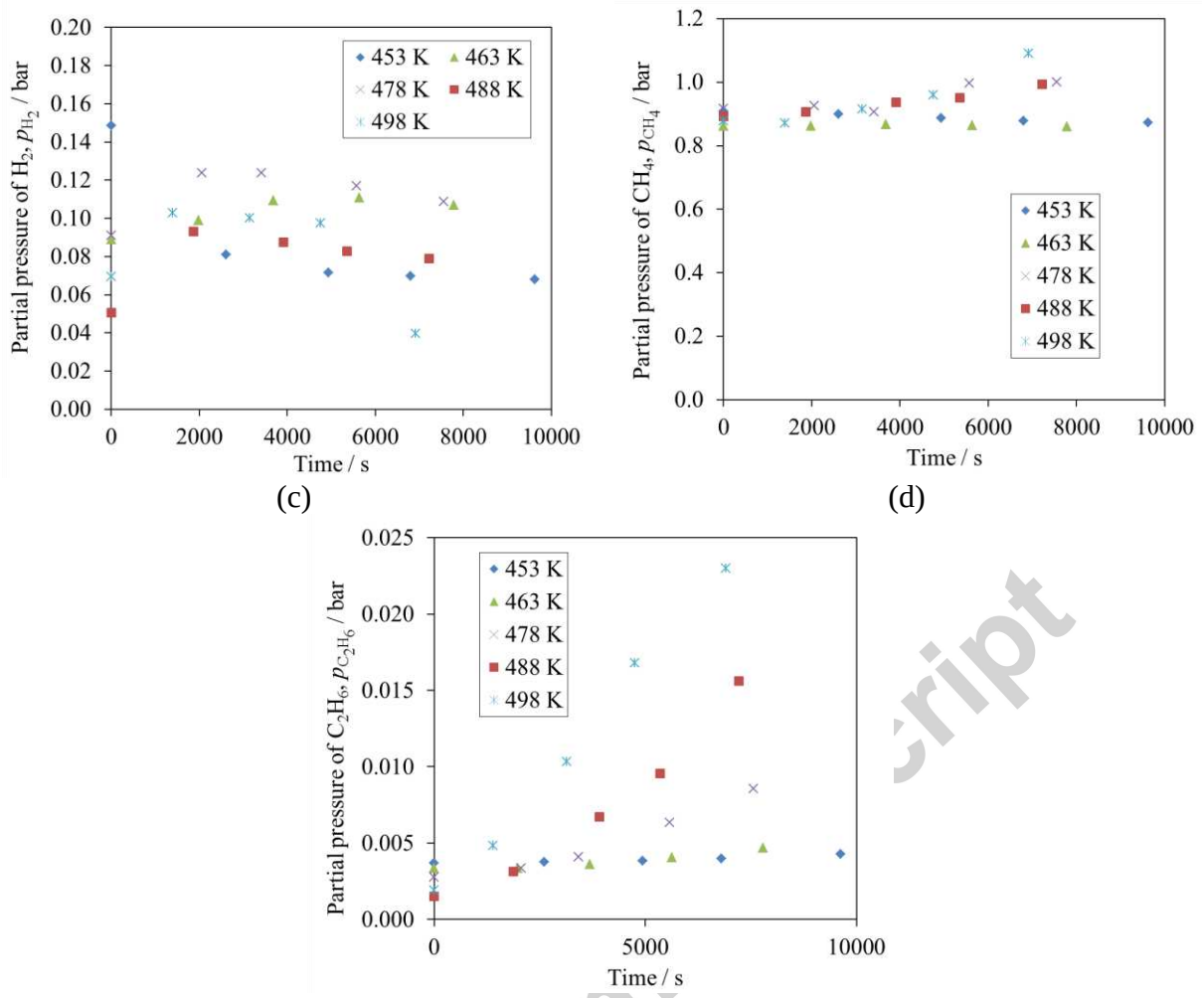

Figure 9. The partial pressure of (a) CO_2, (b) CO, (c) H_2, (d) CH_4 and (e) C_2H_6 as a function of time for different reaction temperatures. For all experiments, $p_{H_2O,0} = 1.8$ bar, $p_{CO,0} = 2$ bar and $m_{cat} = 5.0$ g.

4 Theory

4.1 Reactor model

Section 3.1 has established that reaction (4) occurs simultaneously with the water –gas shift reaction, i.e. reaction (1). The rate of reaction (4) can be taken to be much faster than reaction (1), evident from the low levels of p_{H_2} for all experiments. Hence, for every 2 mole of CO_2 produced, 2 mole of CO were consumed in reaction (1) and an additional mole of CO in reaction (4). The transient changes of p_{CO}, p_{H_2O} and p_{CO_2} in the Carberry reactor were

modelled by the following ordinary differential equations, where the stoichiometry was based on the overall reaction (5) on a basis of 1 mole of CO_2 produced:

$$\frac{dp_{CO}}{dt} = -\frac{1.5 m_{cat} RT}{V_{reactor} \times 10^5} r' \quad 6$$

$$\frac{dp_{H_2O}}{dt} = -\frac{0.5 m_{cat} RT}{V_{reactor} \times 10^5} r' \quad 7$$

$$\frac{dp_{CO_2}}{dt} = \frac{m_{cat} RT}{V_{reactor} \times 10^5} r' \quad 8$$

where p_{CO}, p_{H_2O} and p_{CO_2} are the partial pressures of CO, H_2O and CO_2 in bar, r' represents the rate of reaction(5), taken to be approximately equal that of reaction (1), the water-gas shift reaction, t is in seconds, m_{cat} is the mass of the catalyst in the reactor in grams and $V_{reactor}$ is the volume of the reactor in m^3. Equations (6 – 8) were solved using the initial conditions of the experiments at t = 0 using the MATLAB solver ode45 and for appropriate r', discussed below.

4.2 Kinetic modelling

Two different reaction schemes are presented in this Section. The first scheme, Model I, involves the oxidation of the surface of the catalyst followed by the reduction of the surface, typically known as the redox mechanism (Koryabkina et al, 2003; Li et al., 2000). It should be noted that this scheme was proposed for copper-based catalysts and very little work has been performed on the water-gas shift reaction on nickel-based catalyst, presumably because it is difficult to study the reaction independently of hydrogenation or methanation reactions. The sequence of elementary steps is outlined in Reactions (9) – (12).

$$H_2O + \theta \rightleftarrows \theta_O + H_2 \quad (9)$$

$$CO + \theta \rightleftarrows \theta_{CO} \quad (10)$$

$$\theta_{CO} + \theta_O \rightarrow \theta_{CO_2} + \theta \quad (11)$$

$$\theta_{CO_2} \rightleftarrows CO_2 + \theta \quad (12)$$

A Langmuir-Hinshelwood approach was used to derive a kinetic expression based on the redox mechanism. The active sites for the reaction were assumed to be identical and their

distribution uniform throughout the catalyst pellets. It was assumed that the reaction between surface CO and O, viz. reaction (11), is the rate limiting step. By taking the most abundant species on the surface of the catalyst to be adsorbed CO and H_2O, the following rate expression can be derived:

$$r_{WGS,I} = \frac{a_I\, p_{H_2O}\, p_{CO}}{\left(1 + b_I\, p_{CO} + c_I\, p_{H_2O}\right)^2}. \qquad (13)$$

where a_I, b_I and c_I are kinetic parameters: a_I is a composite of rate and equilibrium constants.

The second model, Model II, assumed that the surface of the catalyst was saturated with adsorbed CO as a result of the strong affinity of CO on the surface of nickel sites (Fujita et al. 1993). As a result, H_2O reacts directly from the gaseous phase with adsorbed CO. This is summarised by reactions (14) and (15).

$$CO + \theta \underset{k_{-1}}{\overset{k_1}{\rightleftharpoons}} \theta_{CO} \qquad (14)$$

$$H_2O + \theta_{CO} \xrightarrow{k_2} CO_2 + H_2 + \theta \qquad (15)$$

The resulting rate expression can be derived:

$$r_{WGS,II} = \frac{a_{II}\, p_{H_2O}\, p_{CO}}{\left(1 + b_{II}\, p_{CO}\right)}. \qquad (16)$$

4.2.1 Model I

Table 1 shows the kinetic parameters obtained by least-squares minimisation (Lim et al. 2016a) of Model I, in conjunction with the reactor model in Section 4.1, with the experimentally-measured profile of the partial pressure of CO_2 with time. Figures 10 and 11 illustrate the goodness of fit between the resulting model, based on Model I, and the experimental results. Figure 10 shows that Model I predicts a general agreement between the modelling and experimental results for initial partial pressures of CO, $p_{CO,0}$, < 1 bar. However, as $p_{CO,0}$ was increased from 1 to 2 bar, the model predicted a decrease in rate, which was not observed experimentally. This effect is the result of the squared-term in the denominator of Eq.(13), where the rate is predicted to decrease at high values of p_{CO}. The agreement between the modelling and experimental results for varying the initial partial pressure of H_2O, $p_{H_2O,0}$, is illustrated in Figure 11. The resulting model predicted that the rate of reaction increases with $p_{H_2O,0}$. Although the agreement between the modelling and the

experimental results is good for low $p_{H_2O,0}$, the model failed to predict the rates of reactions when $p_{H_2O,0}$ = 2.5 and 3.6 bar. The rate of reaction appeared to approach an asymptote, as the predicted rate of increase in the rate of reaction with p_{H_2O} diminished towards high $p_{H_2O,0}$.

Table 1. Kinetic parameters of Model I at 463 K determined by least-squares minimisation.

a_I	b_I	c_I
19.4×10^{-3} mol bar^{-2} s^{-1}	48.4 bar^{-1}	17.6 bar^{-1}

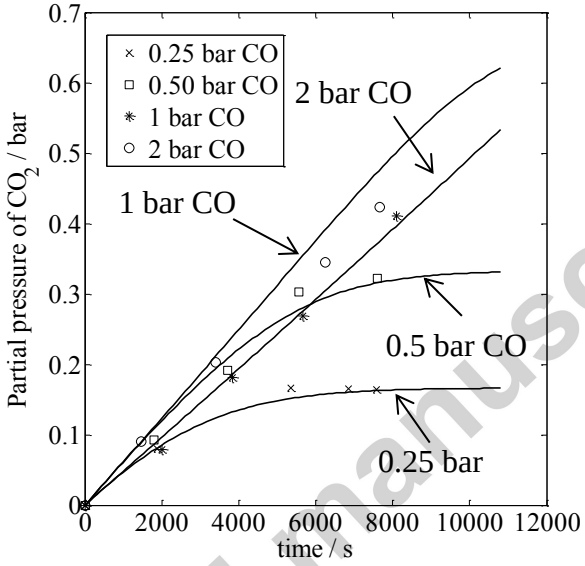

Figure 10. Comparison of the modelling and experimental results for different initial partial pressures of CO. For all experiments, $p_{CO,0}$ = 2 bar, T = 463 K and m_{cat} = 5.0 g. The solid lines represent the modelling results and the symbols the experimentally-measured p_{CO_2}.

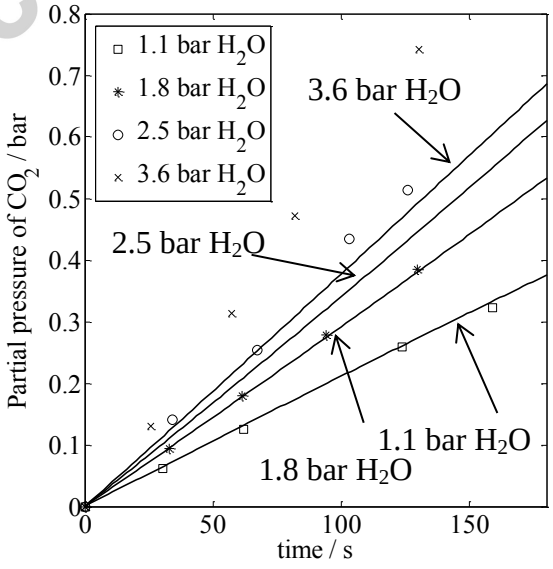

Figure 11. Comparison of the modelling and experimental results for different initial partial pressures of H_2O. For all experiments, $p_{H_2O,0} = 2$ bar, T = 463 K and m_{cat} = 5.0 g. The solid lines represent the modelling results and the symbols the experimentally-measured p_{CO_2}.

4.2.2 Model II

In the derivation of Model II, b_{II} in Eq. (16) represents the equilibrium constant of the adsorption of CO on nickel surfaces. The adsorption of CO has been explored by a number of researchers (Huang and Richardson, 1978; Sehested et al., 2005; Weatherbee and Bartholomew, 1982). Huang and Richardson (1978) performed CO methanation experiments on nickel impregnated into silica-alumina at temperatures 523 – 603 K. Here, Huang and Richardson's (1978) values of b_{II} were extrapolated to lower temperatures of 453 – 498 K. The variation of b_{II} with temperature was expressed as

$$b_{II} = 1.13\times10^{-3}\exp\left(\frac{42700}{RT}\right)\ \text{bar}^{-1}. \qquad (17)$$

With the value of b_{II} pre-determined, least-squares minimisation was performed to determine the value of a_{II} at different temperatures using the variation of p_{CO_2} with time for different initial conditions. The resulting parameters are given in Table 2. Figures 12, 13 and 14 illustrate the agreement between Model II and the experimental results at 453, 463 and 488 K. Figure 15 illustrates the change in p_{CO_2} with time at different temperatures for $p_{CO,0} = 2$ bar and $p_{H_2O,0} = 1.8$ bar. In general, there is excellent agreement between the modelling and the experimental measurements. The apparent activation energy of a_{II} was estimated to be -47 ± 5 kJ mol^{-1} using the gradient of straight line fit of the logarithm of a_{II} against the reciprocal of time. The parameter a_{II} is a composite of the rate parameter of reaction (15), k_2, and the equilibrium constant of CO which is b_{II}. The variation of a_{II} with temperature is

$$a_{II} = 42.7\exp\left(-\frac{47200}{RT}\right). \qquad (18)$$

Therefore, k_2 can be expressed as

$$k_2 = \frac{a_{II}}{b_{II}} = 37.78\exp\left(-\frac{90000}{RT}\right). \qquad (19)$$

Table 2. Kinetic parameters of Model II at different temperatures.

T / K	a_{II} / mol bar^{-2} s^{-1}	b_{II} / bar^{-1}
453	1.6×10^{-4}	94
463	2.0×10^{-4}	74
478	3.0×10^{-4}	52
488	3.7×10^{-4}	42
498	5.0×10^{-4}	34

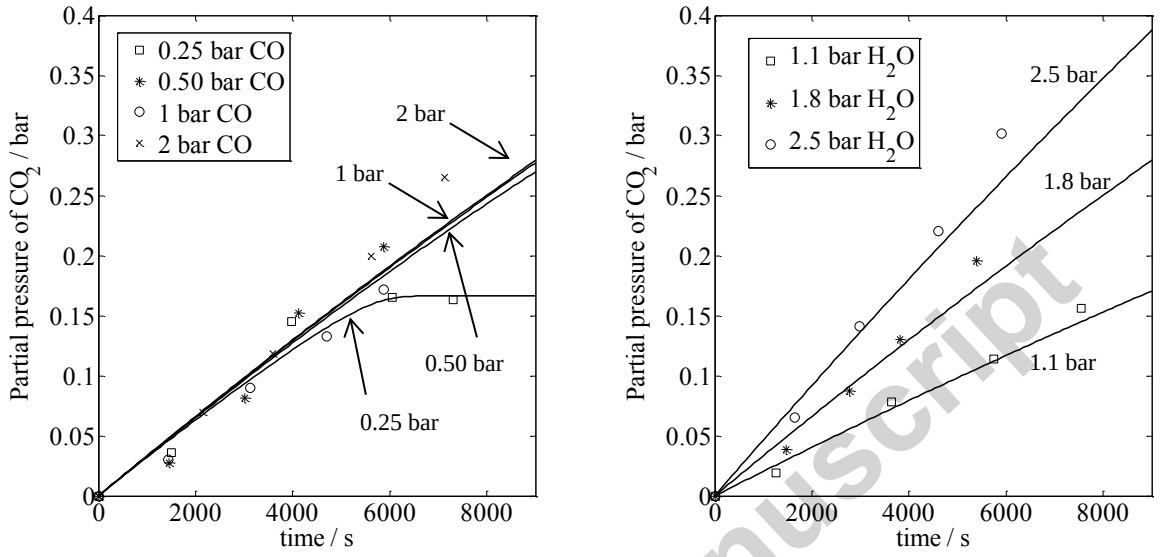

(a) (b)

Figure 12. The experimental measurements and the modelling results of the partial pressure of CO_2 with time for (a) different $p_{CO,0}$ with $p_{H_2O,0}$ = 1.8 bar and (b) different $p_{H_2O,0}$ with $p_{CO,0}$ = 2 bar. For all cases, T = 453 K and m_{cat} = 5.0 g.

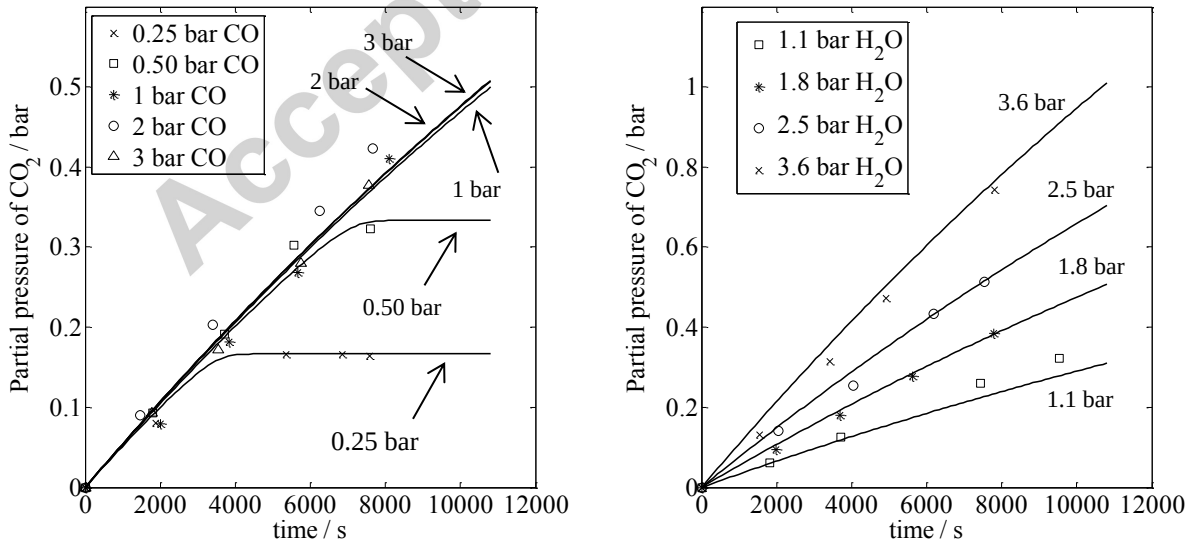

(a) (b)

Figure 13. The experimental measurements and the modelling results of the partial pressure of CO_2 with time for (a) different $p_{CO,0}$ with $p_{H_2O,0}$ = 1.8 bar and (b) different $p_{H_2O,0}$ with $p_{CO,0}$ = 2 bar. For all cases, T = 463 K and m_{cat} = 5.0 g.

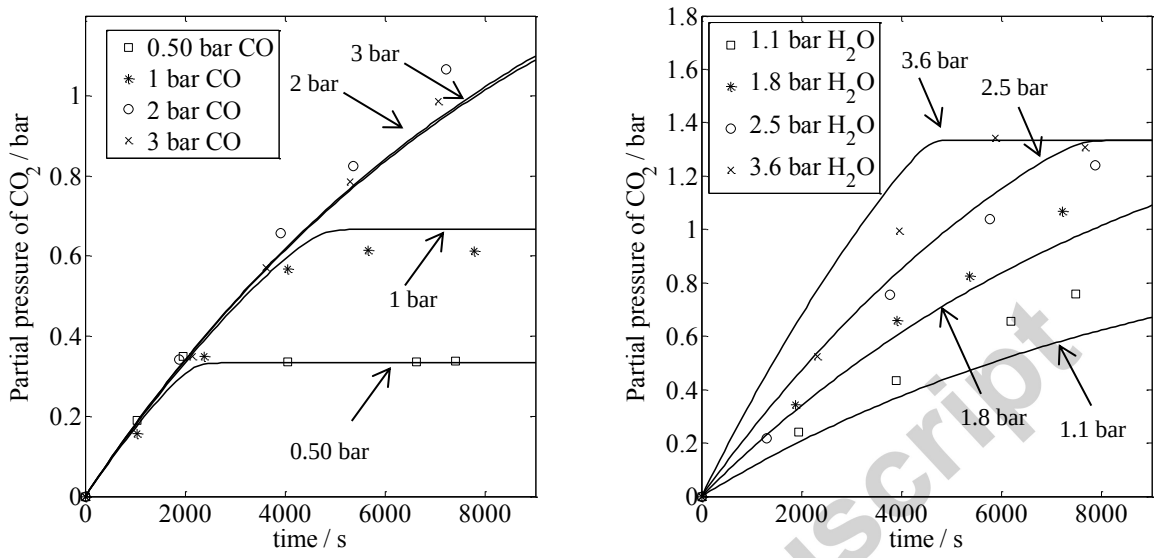

(a) (b)

Figure 14. The experimental measurements and the modelling results of the partial pressure of CO_2 with time for (a) different $p_{CO,0}$ with $p_{H_2O,0}$ = 1.8 bar and (b) different $p_{H_2O,0}$ with $p_{CO,0}$ = 2 bar. For all cases, T = 488 K and m_{cat} = 5.0 g.

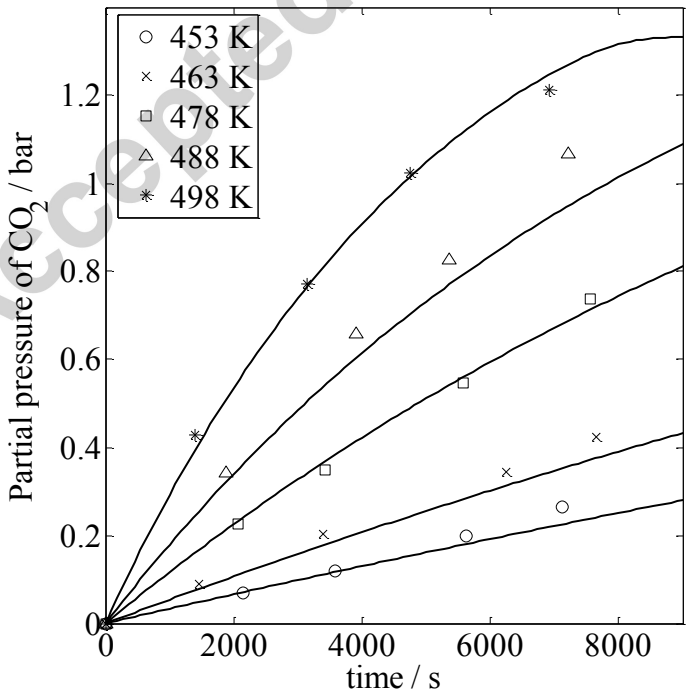

Figure 15. The comparison of modelling and experimental results for the partial pressure of CO_2 versus time at different reaction temperatures, for $p_{CO,0} = 2$ bar, $p_{H_2O,0} = 1.8$ bar and m_{cat} = 5.0 g. The symbols represent the experimental results and the solid lines were evaluated based on Model II.

5 Discussion

As noted in Section 3.2, a higher partial pressure of H_2O increased the rate of the water-gas shift reaction over the Ni/γ-Al_2O_3 catalyst. However, the rate was largely constant for variations in the partial pressure of CO for p_{CO} > 0.1 bar, as illustrated in Figure 8 (a). The transition from a constant rate regime to zero rate occurred very abruptly. Hence, the threshold of p_{CO} when the transition occurred is only an estimate. There are very few studies of the water-gas shift reaction in the literature performed on nickel-based catalysts at temperatures below 488 K. This might be the result of (i) the low activity of the water-gas shift reaction over nickel based catalysts at low temperatures and (ii) the high selectivity of the catalyst towards hydrogenation reactions normally resulting in the water-gas shift reaction taken merely as a side reaction in an investigation. Li et al. (2000) investigated the water-gas shift reaction from 523 – 573 K using a nickel catalyst supported on a ceria oxide doped with La. Their experiments were performed using an atmospheric-pressure, quartz tubular reactor and explored the partial pressures of CO up to only 0.03 bar. In general, they found a small increase in the rate of reaction which appeared to approach an asymptote. This is consistent with the experimental observations in this paper. However, because the partial pressure of CO used in the batch reactor in the present research was very much higher than those of Li et al. (2000), the direct comparison of the experimental measurements is difficult. Furthermore, there was no indication by Li et al. (2000) whether or not their catalyst was active in hydrogenation reactions.

It is clear that Model I, derived from the redox mechanism, does not describe the experimental observations of the production of CO_2 from the water-gas shift reaction over the Ni/γ-Al_2O_3 catalyst in a batch reactor. This is not unexpected since the redox mechanism has been shown to describe the kinetics of the water-gas shift reaction on copper-based - rather than nickel-based - catalysts (van Herwijnen and de Jong, 1980; Koryabkina et al., 2003; Li et al., 2000). Studies using Cu have explored the rate of reaction at low partial pressures of CO and H_2O. For example, Koryabkina et al. (2003) studied the water-gas shift reaction over a CuO-ZnO/Al_2O_3 catalyst over a range of p_{H_2O} of 0.17 – 0.38 bar and p_{CO} of 0.06 – 0.20 bar at 463 K and found the rate of reaction increased with p_{H_2O} and p_{CO}. The values of

p_{H_2O} and p_{CO} used in this paper (up to 3 bar CO and 3.6 bar H_2O) were an order of magnitude larger than the those studied by Koryabkina et al. (2003).

Section 4.2.2 has shown that Model II, based on an Eley-Rideal mechanism, is in good agreement with the experimental results over a large range of p_{H_2O} and p_{CO}. The modelling results also provided evidence that the overall stoichiometry is consistent with reaction (5), illustrated by the final value of p_{CO_2} when p_{CO} was depleted in Figures 13(a) and 14(a). If the stoichiometry of the water-gas shift reaction, i.e. reaction (1), were used in the reactor model in Section 4.2.2, the final amount of p_{CO_2} at the end of the batch experiment would be higher because p_{CO} would have taken longer to be depleted. This provides evidence that hydrogenation reactions were occurring at a rate much faster than the water-gas shift reaction; an observation confirmed by Lim et al. (2016b). It should be noted that Huang and Richardson (1978) determined the equilibrium constant for CO on supported nickel catalyst and this was used in b_{II} of Model II, based on CO methanation experiments, where the effects of the adsorption of CO plays an important role in CO methanation. Since it has been established that reactions (1) and (4) occur simultaneously, it is reasonable to use the values of b_{II} determined by Huang and Richardson (1978) in the present study. Furthermore, the variation of a_{II} was found to obey the Arrhenius relationship with an apparent activation energy of 42.7 ± 5 kJ mol^{-1}, in good agreement with the range of apparent activation energies of 30 to 80 kJ mol^{-1} reported for different catalysts in the literature (Grenoble et al., 1981; Li et al., 2000). In a number of cases in Figures 12 to 15, the model slightly underpredicts the experimental results. One possible reason for this is that we have used Huang and Richardson's (1978) result for values of $b_{II,}$ extrapolated to our lower temperatures of 453 – 498 K. It is unlikely that the catalyst used in the present work was an exact copy of Huang and Richardson's (1978) and so it is probable that $b_{II,}$ might have actually been slightly different to the value given by Eq. (17). This is a direction for further investigation.

6 Conclusions

The Boudouard and water-gas shift reactions were studied over a Ni/γ-Al_2O_3 catalyst in a Carberry reactor in batch using different mixtures of CO, H_2 and CO_2. The rate of the Boudouard reaction was found to be low, compared to the water-gas shift reaction, and diminished over time, suggesting that the temperature was too low for significant activity after an initiation period of CO adsorption. Furthermore, the rate of the Boudouard reaction

has been reported to decrease in the presence of H_2O and H_2. The water-gas shift reaction was found to be the main reaction responsible for the production of CO_2 in a mixture of CO, H_2 and H_2O in the batch reactor. The ratio of the total amount of CO consumed to the total amount of CO_2 produced showed that the catalyst was also active in hydrogenation, where the rate of the hydrogenation reaction was very much faster than the water-gas shift reaction. The resulting ratio of p_{H_2} to p_{CO} was found to be extremely low, probably leading to the production of long-chain hydrocarbons. The stoichiometry of the overall reaction was such that for every mole of mole of CO_2 produced, 1.5 mole of CO was consumed in the batch reactor.

Kinetic studies were performed on the batch reactor at different temperatures between 453 and 488 K by varying the initial partial pressures of CO and H_2O in the batch reactor. In general, the rate of reaction was higher at higher p_{CO}. However, there was little variation in the rate of reaction for $p_{CO} > 0.1$ bar for all temperatures and p_{H_2O}. Model II, based on an Eley-Rideal mechanism, was found to provide a good agreement with the experimental results over a wide range of p_{H_2O} and p_{CO}. This mechanism is consistent with the strong affinity of CO for nickel sites.

Acknowledgements

JYL was funded by the Cambridge International Scholarship Scheme. The Cambridge Philosophical Society, the Lundgren Research Award and Corpus Christi College are also gratefully thanked for contributing to the support of his PhD studies. We are grateful for the assistance of Dr A.P.E. York, Johnson Matthey Technology Centre, Sonning Common, Reading RG4 9NH, United Kingdom, for his valuable input to this research.

References

Fujita, S. I., Nakamura, M., Doi, T., Takezawa, N. (1993). Mechanisms of methanation of carbon dioxide and carbon monoxide over nickel/alumina catalysts. Applied Catalysis A: General, **104** (1), 87-100.

Gardner, D. C., Bartholomew, C. H. (1981). Kinetics of carbon deposition during methanation of carbon monoxide. Industrial & Engineering Chemistry Product Research and Development, **20** (1), 80-87.

Grenoble, D. C., Estadt, M. M., Ollis, D. F. (1981). The chemistry and catalysis of the water gas shift reaction: 1. The kinetics over supported metal catalysts. Journal of Catalysis, **67** (1), 90-102.

Huang, C. P., & Richardson, J. T. (1978). Alkali promotion of nickel catalysts for carbon monoxide methanation. Journal of Catalysis, **51** (1), 1-8.

Lemmon, E. W., McLinden, M. O., Friend, D. G. Thermophysical Properties of Fluid Systems. In NIST Chemistry WebBook, NIST Standard Reference Database Number 69; Linstrom, P.J., Mallard, W. G., Eds.; National Institute of Standards and Technology: Gaithersburg MD, 20899. http://webbook.nist.gov. (retrieved 15th February, 2014).

Li, Y., Fu, Q., Flytzani-Stephanopoulos, M. (2000). Low-temperature water-gas shift reaction over Cu-and Ni-loaded cerium oxide catalysts. Applied Catalysis B: Environmental, 27 (3), 179-191.

Lim, J.Y., McGregor, J., Sederman, A.J., York, A.P.E. and Dennis, J.S. (2016a). Kinetic studies of CO_2 methanation using a batch reactor over a Ni/γ-Al_2O_3 catalyst. Chemical Engineering Science, **141**, 28-45.

Lim, J.Y., McGregor, J., Sederman, A.J., York, A.P.E. and Dennis, J.S. (2016b). Kinetic studies of CO methanation using a batch reactor over a Ni/γ-Al_2O_3 catalyst. Chemical Engineering Science, http://dx.doi.org/10.1016/j.ces.2016.02.001i.

Rostrup-Nielsen, J., Trimm, D. L. (1977). Mechanisms of carbon formation on nickel-containing catalysts. Journal of Catalysis, **48** (1), 155-165.

Rostrup-Nielsen, J. R. (1972). Equilibria of decomposition reactions of carbon monoxide and methane over nickel catalysts. Journal of Catalysis, **27** (3), 343-356.

Sehested, J., Dahl, S., Jacobsen, J., Rostrup-Nielsen, J. R. (2005). Methanation of CO over nickel: Mechanism and kinetics at high H_2/CO ratios. The Journal of Physical Chemistry B, **109** (6), 2432-2438.

Tøttrup, P. B. (1976). Kinetics of decomposition of carbon monoxide on a supported nickel catalyst. Journal of Catalysis, **42** (1), 29-36.

Xu, J., Froment, G. F. (1989). Methane steam reforming, methanation and water-gas shift: I. Intrinsic kinetics. AIChE Journal, **35** (1), 88-96.

Highlights

- Both reactions investigated in a spinning-basket reactor operated in batch
- Rate and selectivity determined for 12 wt% Ni/γAl_2O_3 catalyst, 453 and 490 K to 16 bar
- Rate of Boudouard reaction much less than that of water-gas-shift (WGS)
- WGS was main reaction responsible for the production of CO_2 in a mixture of CO, H_2 and H_2O in the reactor
- Eley-Rideal mechanism accounted for the experimental results over a wide range of partial pressures of steam and CO